ARGONNE NATIONAL LABORATORY

ANL-Gen IV-054

Generation IV Nuclear Energy System Initiative Status Report: Guard Containment CFD Analysis

prepared by
Nuclear Engineering Division
Argonne National Laboratory

Argonne National Laboratory is managed by
The University of Chicago for the U. S. Department of Energy

Availability of This Report
This report is available, at no cost, at http://www.osti.gov/bridge. It is also available on paper to the U.S. Department of Energy and its contractors, for a processing fee, from:

U.S. Department of Energy
Office of Scientific and Technical Information
P.O. Box 62
Oak Ridge, TN 37831-0062
phone (865) 576-8401
fax (865) 576-5728
reports@adonis.osti.gov

ANL-Gen IV-054

Generation IV Nuclear Energy System Initiative Status Report: Guard Containment CFD Analysis

by
C.P. Tzanos
Nuclear Engineering Division, Argonne National Laboratory

September 2005

Argonne National Laboratory is managed by
The University of Chicago for the U. S. Department of Energy

Table of Contents

List of Figures

List of Tables

1.0 Introduction

Under the auspices of the CEA Cadarache/ANL-US I-NERI project a comprehensive investigation has been made of improvements to the Gen-IV GFR safety case over that of the GCFR safety case twenty five years ago. In particular, it has been concluded and agreed upon [1] that the GFR safety approach for the passive removal of decay heat in a protected depressurization accident with total loss of electric power needs to be different from that taken for the HTRs. The HTR conduction cooldown to the vessel wall boundary mode for an economically attractive core is not feasible in the case of the GFR because the high power densities (100kW/1 compared to 5 kW/1 for pebble bed thermal reactor) require decay heat fluxes well beyond those achievable by the heat conduction and radiation heat transfer mode. A set of alternative novel design options has been evaluated for potential passive safety mechanisms unique to the GFR. In summary, from a technological risk viewpoint and R&D planning, the option which has been identified is the block/plate-based or a pin-based reactor with a secondary guard containment/vessel around the primary vessel to maintain the primary system pressure at a high enough level which would allow primary system natural convection removal of core generated decay heat to be effective. Dedicated emergency decay heat exchangers would have to be connected in a "failure-proof" configuration to the primary system and have natural convection capability all the way to the ultimate heat sink.

What has been collaboratively agreed upon and selected for further development is the natural convection option with a block/plate or pin type derated core and a hybrid passive/active approach.[2] The guard containment will be utilized but it will be sized for an LWR containment range backup pressure (5-7 bars) with an initial pressure of 1 bar. The assessment has shown that a significantly higher back pressure is required for total natural convection driven removal of significant decay heat levels at GFR target power densities. The lower back-up pressure, plus whatever natural convection is available at this pressure, will be utilized to significantly reduce the blower power of the active DHR system sized to remove 2-3% decay power. The objective is to be able to have such low power requirements so that power supplies such as batteries without the need for startup, can be utilized. This lower back-up pressure should be sufficient to support natural convection removal of 0.5% decay heat which occurs at ~24 hrs. So there should be no more need for active systems/power supply after the initial period of one day. Furthermore, since there will be a decay of the after-heat from 2-3% to 0.5% in this time period, credit should be taken in probability space for loss of active systems during the 24 hours. The safety approach will then be a probabilistic one. In the future discussions with the regulatory authorities the approach which will then be taken is that this class of decay heat removal accidents should be treated in combination with the PRA rather than solely through deterministic calculations. Work is now ongoing in the U.S.-France I-NERI GFR project to further evaluate this hybrid passive/active approach to heat removal for depressurized decay heat accidents.

The objective of the analysis documented in this report is to provide information on local and global temperature, pressure and flow distributions in the guard containment , during steady state, and reactor vessel depressurization conditions due to a small break in the reactor vessel bottom control rod drive system. This is for the 2400 MWt plant option. The results should lead to improved guard containment designs and enhanced margin for safety criteria.

2.0 2400 MWt Plant Layout

For the 2400MWt GFR core, the Guard Containment (GC) option with a 5bar containment pressure in a pre-stressed concrete containment was selected. The volume and cost analysis described in [2] showed that, at these lower pressures, the GC option has a lower cost than the corresponding pre-stressed concrete reactor vessel (PCRV), which is similar to that used for the FSV reactor, and planned for the GCFR design. This GC option is shown in elevation view in Figure 1. The pre-stressed concrete containment is 36m in diameter and 44m high (other dimensions are also indicated on the figure). The PCU is located outside the Guard Containment, and the GC penetrations for connecting to the PCU and SCS ducts must be separated 4.5m vertically and 1m horizontally to meet ASME code. Use of a smaller spacing leads to a thicker GC wall, and to fabrication problems.

The layout of the 2400MWt direct cycle GC option is given in Figures 1 and 2, which shows the location of the four PCU and four SCS vessels. The overall plant dimensions are driven by the reactor vessel (RV) and PCU requirements. In turn the RV radial dimensions are based upon the core diameter, and the reflector and shielding thicknesses needed. The RV height is based on the SCS height and ducting, the IHX height and location, the core height, the PCU cross vessel location, and refueling reach concerns.

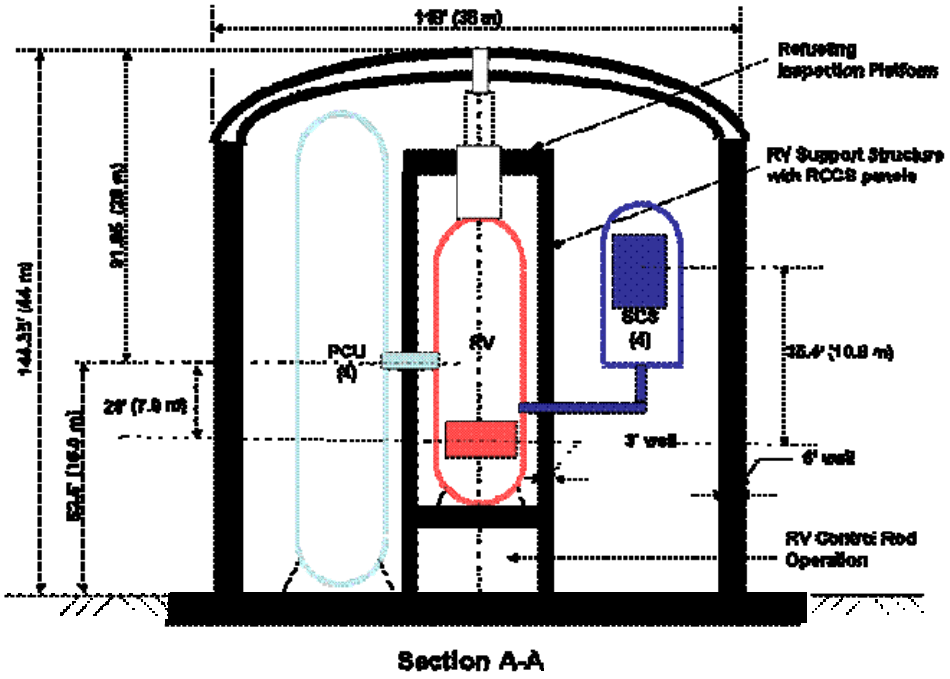

Fig. 1. 2400MWt Guard Containment Elevation View

…….36m (118ft) OD, 1.8m (6ft) thick….

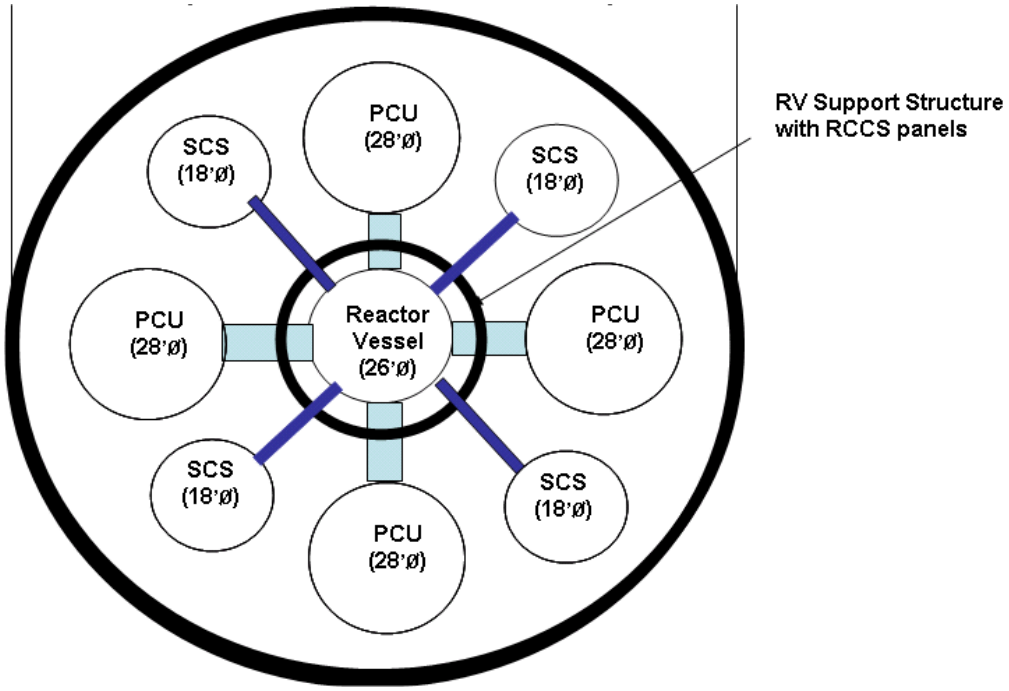

Fig. 2. 2400MWt Plant Layout, Direct Cycle GC Option

3.0 Decay Heat Accidents [2]

A series of transient analysis using the system code RELAP5/ATHENA has been performed by BNL [2] to assess decay heat removal by natural circulation cooling under postulated accident conditions. The analysis is for a helium cooled reactor of pin core design with a power density of 100 W/cc and a thermal power of 2400 MW. The objective is to ensure that the maximum fuel temperature remains within acceptable limits (< 1600°C) following a depressurization accident with scram and total loss of AC power. The break is a postulated small one inch leak in the primary system boundary.

The removal of decay heat from the core will follow the initiation of the depressurization accident in two steps. Initially, heat will be removed by a combination of flow coastdown due to inertia of the power conversion system and system depressurization caused by coolant flowing out of the break from the primary system. Following this step a self-sustaining method for long-term heat removal of the core will be required. A passive mode of heat removal relying on natural circulation cooling is investigated in this report. An emergency heat exchanger loop outside the reactor vessel will transfer energy from the reactor to an ultimate heat sink located outside the guard containment. By the opening of a check valve inline with the emergency heat exchanger a natural circulation flow path is established through the core and between the upper plenum and downcomer of the reactor vessel. Radiative heat transfer has also been included in the model to account for the exchange of thermal energy between heat structures by radiation. In order for natural circulation cooling to function efficiently the primary system and the containment will need to be pressurized to ensure a sufficiently high coolant density. This is accomplished by having a guard containment structure around the primary system. The main objective of the RELAP5 accident analyses is to evaluate the effects of guard containment back pressure on the effectiveness of natural circulation cooling.

A RELAP5 model of the reactor system has been constructed to address differ
ent parametric effects that influence the steady state and transient behavior of the pin core under natural circulation cooling at decay heat power levels. The model consists of two power conversion unit loops, an emergency heat exchanger loop with its heat sink, and a guard containment surrounding the primary system. The actual power plant will be constructed using four power conversion loops. However, in the RELAP model three loops are combined into one large loop (1800 MW), and one loop (600 MW) is isolated in order to correctly model the depressurization dynamics, since the leak flow will emanate from only one of the power conversion loops. Transient history results for break flow mass rate and thermodynamic conditions were obtained with this RELAP5 model for the selected depressurization accident. These histories together with boundary temperatures on the vessel and the DHR were provided to the CFD calculation as forcing functions. The results from the CFD analyses of the guard containment condition and flow distribution patterns will provide insight and guidance for the RELAP5 lumped parameter nodalization of the guard containment. This symbiosis should lead to a better understanding of the system pressure transient.

4.0 Guard Containment CFDModel

The GFR containment is a very large structure, having a radius of 18 m and a height of 44 m. In addition to the reactor vessel, there are many other components inside the containment. The largest ones are four Power Conversion Units (PCUs), four Shutdown Cooling Systems (SCSs), the Reactor Cavity Cooling System (RCCS), and concrete structures that support the reactor vessel. The CFD simulation of this large system is quite challenging. Especially challenging is the analysis of a reactor vessel depressurization transient. This involves spatial and time scales that vary by many orders of magnitude. To meet the challenge, the problem is simplified by neglecting geometrical features whose impact on the fluid dynamics of the system is small, and by using boundary conditions that remove large variations that occur in small space regions and for a short time. A simplified STAR-CD CFD model of the guard containment was developed based on the gross 1/8 symmetry of the containment space. Figure 3 shows the grid of the in-containment fluid space on a horizontal (x-y) plane at a height where the inner and outer cavities communicate. Figure 4 shows a view of the model from the y+ direction. The yellow color represents the containment walls. The green represents the inner cavity, and the purple the outer cavity. The cylindrical wall is the outer wall of one half of a PCU unit. The inner cavity has a RCCS surrounding the reactor vessel with a number of "windows" about the reactor head to allow communication with the outer cavity. The support structure is a concrete cylinder between the two cavities. Figure 5 shows a view of the model from the y- direction. The cylindrical wall represents the outer wall of one half of an RCCS unit. The figure also shows the communication "window" between the inner and outer cavity. The inner boundary of the inner cavity is defined by the outer wall of the reactor vessel. Finally, Figs. 6 & 7 side by show vertical cutaways through the PCU and the DHR cooler. The center lines are through the reactor vessel in both figures. The reactor vessel can be seen in the silhouette outline sitting on top of the control rod room. The lighter outside boundary is the concrete guard containment.

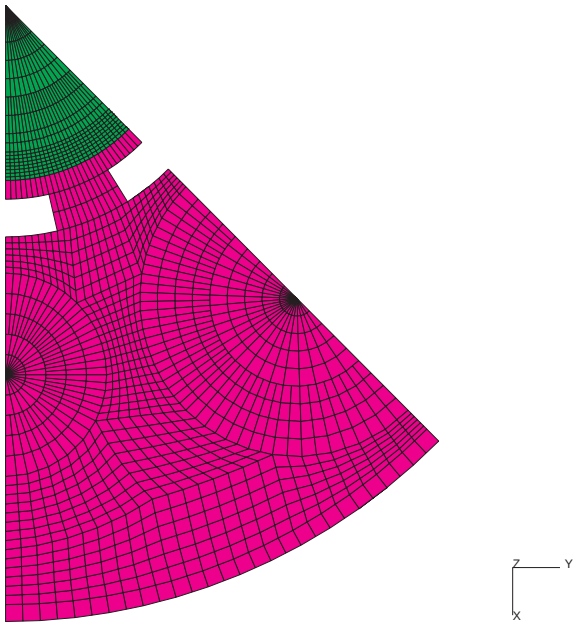

Fig. 3. Grid on A Horizontal Cross-Section

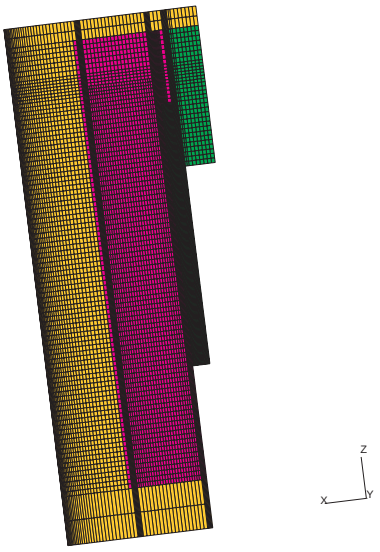

Fig. 4. Grid View from y+

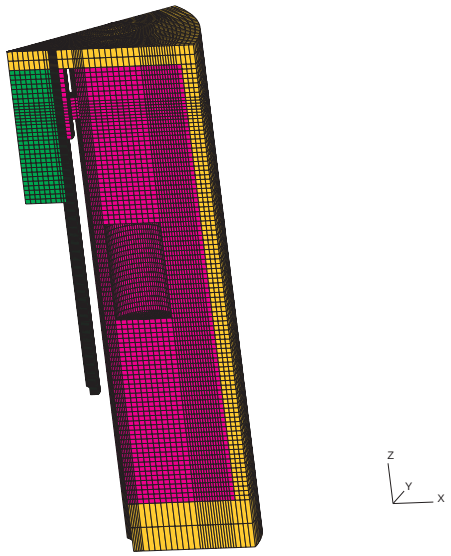

Fig. 5. Grid View from y-

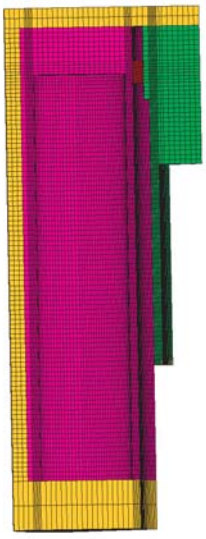

Fig. 6. Vertical Cutaway Though the PCU

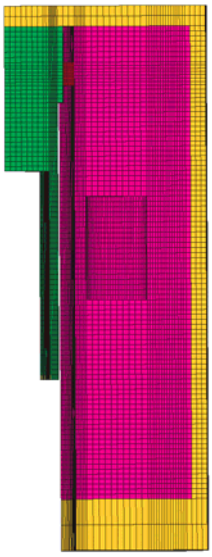

Fig. 7. Vertical Cutaway Through the DHR Cooler

5.0 Long Term Steady State Analysis

A steady state analysis was performed at the conditions prevailing at the end of the depressurization transient as determined by the RELAP analysis. This is the long term steady state as the accident reaches a quasi-equilibrium. The temperature boundary conditions used for this analysis are: 303 ° K (30 °C) on the outer wall of the containment; 335 ° K (62 °C) on the outer wall of the RCCS unit; 338.6 ° K (65.6 °C) on the outer boundary of the inner cavity, the boundary of the "window", the inner boundary of the outer cavity, and the bottom boundary of the inner cavity; 490 ° K (217 °C) on the lower 10.6 m of the reactor vessel wall; 520 ° K (247 °C) on the upper section and on the top of the reactor vessel; and an adiabatic condition on the outer wall of the PCU unit. An emissivity of 0.7 was used for all radiating surfaces. The containment atmosphere is composed of a mixture of nitrogen (75% mol fraction) and helium (25% mol fraction) at a pressure of 6 bar which within the range of 5-7 bar.

The model did not converge to a steady state. This may be due to the very weak coupling of the natural convection flows in the inner and outer cavity through the small "window" in the upper part of the containment space.

Figure 8 shows the temperature distribution in the containment fluid (nitrogen-helium mixture). As expected the hotter region is the area around the vertical side of the reactor vessel, which reaches a maximum temperature of 412 ° K (139 °C). Most of the outer cavity has a temperature of about 348 ° K (75 °C). Figure 9 shows the temperature of the containment wall. The maximum temperature occurs on the inner surface above the reactor vessel, which reaches a temperature of 350 °K (77 °C).

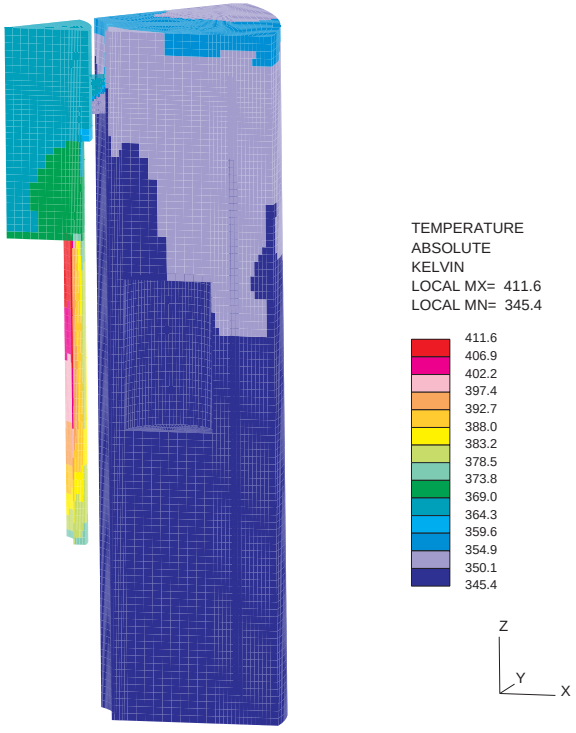

Fig. 8. Fluid Temperature

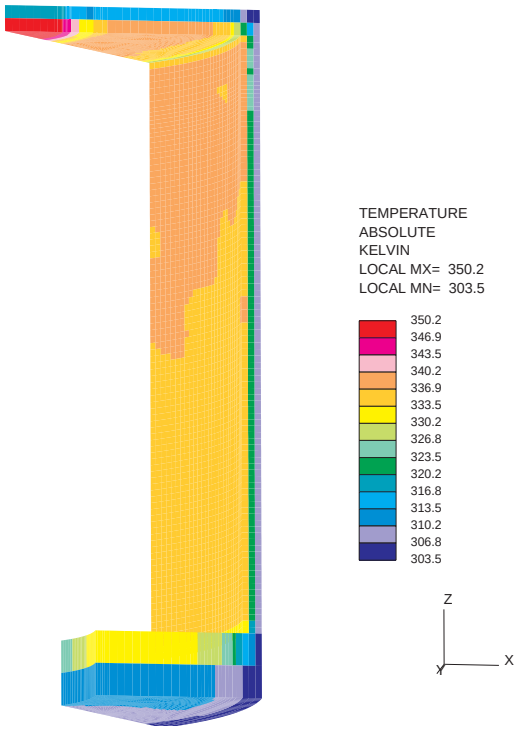

Fig. 9. Temperature of Containment Structure

Figures 10 and 11 are the side-by-side mirror reflection of Figures 6 and 7and they show the flow distribution patterns in these areas at the long term steady state. Figures 12, and 13 show the flow on two vertical planes in the section of the inner cavity above the reactor vessel. Its main feature is two large vortices rotating in opposite directions. As a continuation of Figure 12, Figure 14 shows the main flow pattern in the inner cavity below the top of the reactor vessel: the gas flows up along the hot wall of the reactor vessel and down along the cold outer wall of the inner cavity.

Figure 15 shows the flow through the "window" that provides communication between the inner and outer cavity. Fluid flows from the hot inner cavity to the cold outer cavity in the upper section of the window, while cold gas from the outer cavity flows to the inner cavity through the lower section of the window. The air velocities in the outer cavity are lower than in the inner cavity and the flow patterns are quite complex. Figure 16 shows the flow on a vertical plane passing through the axis of the outer cavity. Figures 17 to 20 show the flow in sections of the outer cavity.

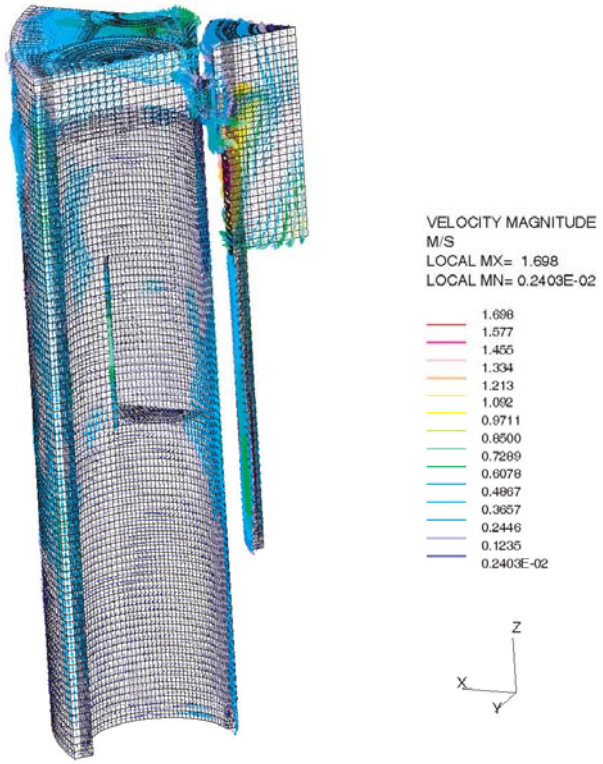

Fig. 10. Flow Distribution in DHR Cutaway

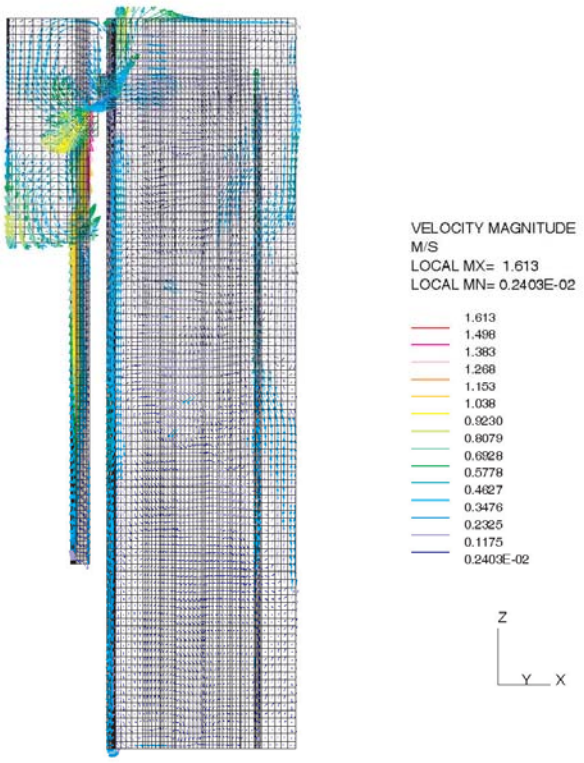

Fig. 11. Flow Distribution in PCU Cutaway

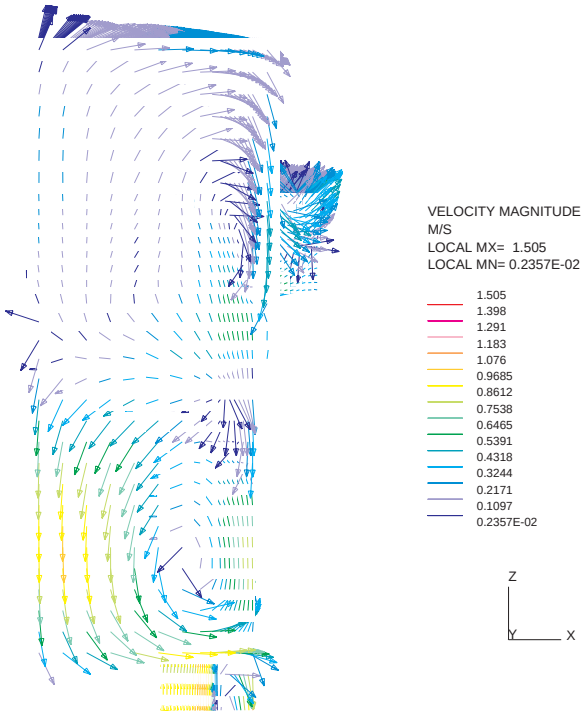

Fig. 12. Flow in the Inner Cavity, Above the Reactor Vessel (Section 1)

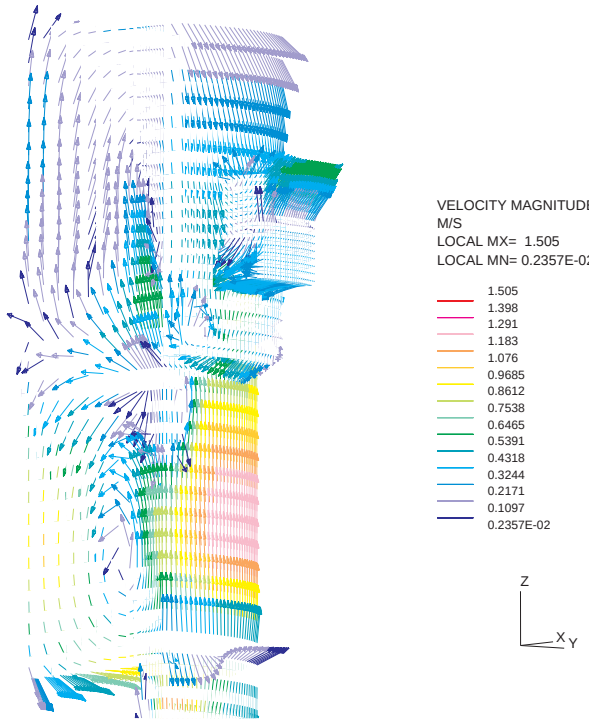

Fig. 13. Flow in Inner Cavity, Above the Reactor Vessel (Section 2)

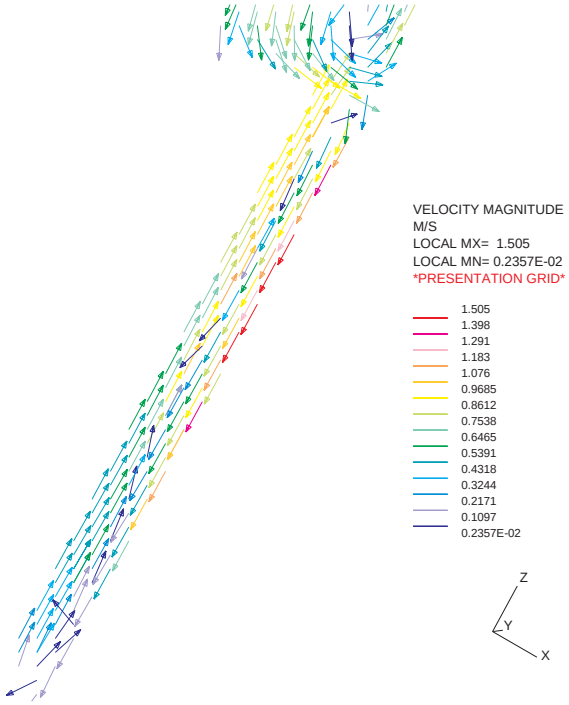

Fig. 14. Flow in The Inner Cavity, Below The Top of the Reactor Vessel

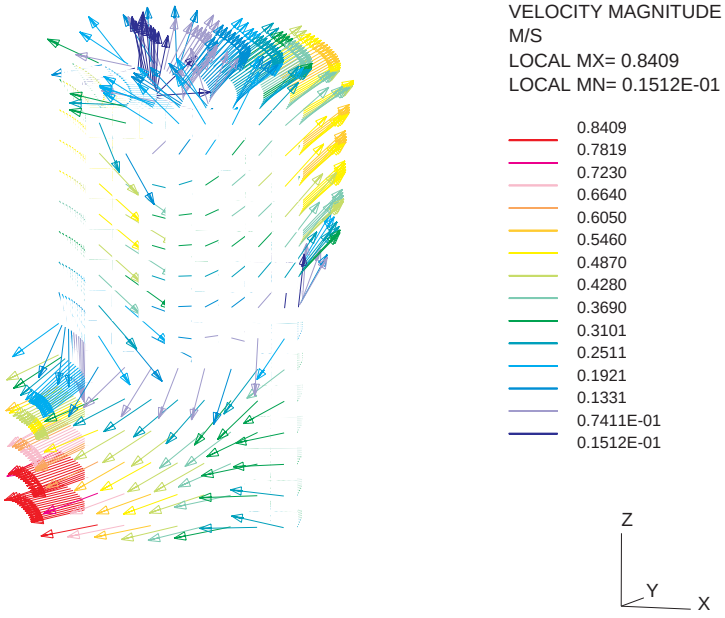

Fig. 15. Flow Through the "window"

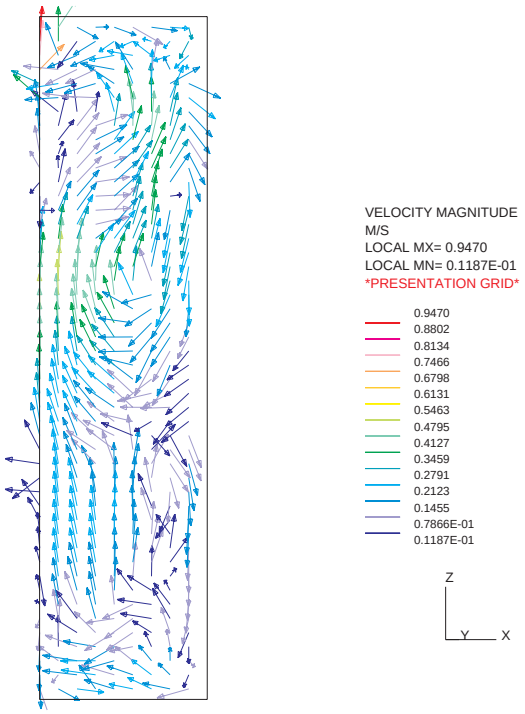

Fig. 16. Flow in the Outer Cavity on A Vertical Plane Passing through the Cavity Axis of Symmetry

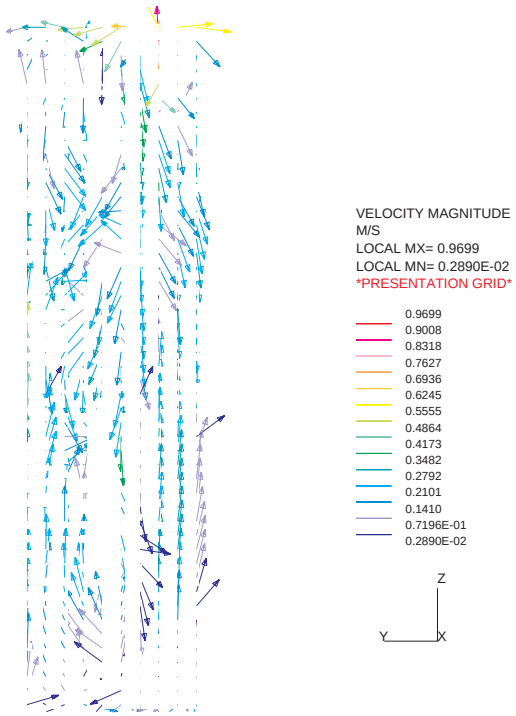

Fig. 17. Flow in the Outer Cavity (view from x-)

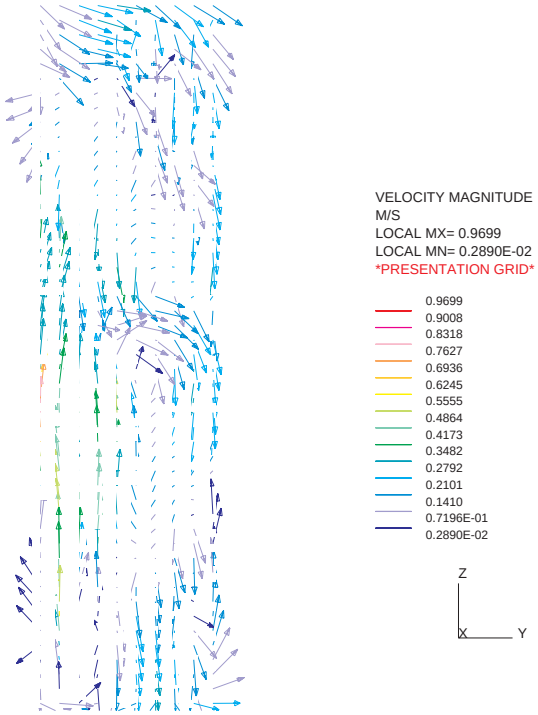

Fig. 18. Flow in the Outer Cavity (view from x+)

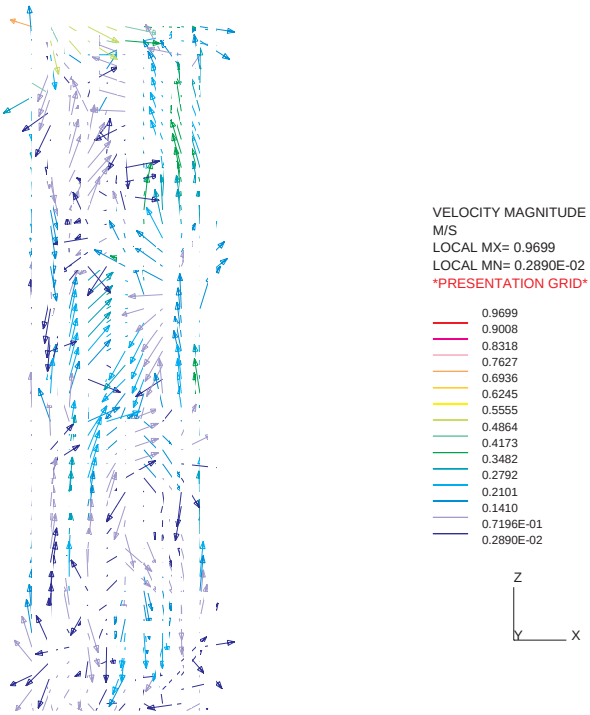

Fig. 19. Flow in the Outer Cavity (view from y-)

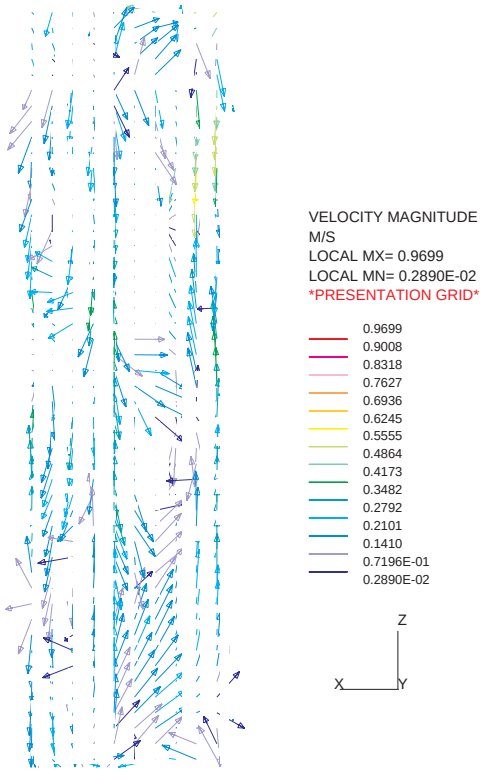

Fig. 20. Flow in the Outer Cavity (flow from y+)

Table 1 gives the convective heat flux for each inner boundary of the system, and Table 2 gives the radiative heat flux for the same boundaries.

Table 1. Average Convective Heat Flux, w/m^2

Boundary Surface	**Heat Flux**
Reactor vessel – lower vertical wall	1884.30
Reactor vessel – upper vertical wall	3137.00
Reactor vessel top	4444.50
Inner surface of containment top – inner cavity	-32.00
Inner cavity floor	-261.90
Inner cavity vertical outer boundary	-886.00
Inner vertical surface of outer containment wall	-33.29
Inner surface of containment top – outer cavity	-61.10
Containment floor – outer cavity	-18.82
Inner boundary of outer cavity	-107.06
Vertical surface of SCS	-98.12
Top of SCS	-71.45
Bottom SCS	-60.66

Table 2. Radiactive Heat Flux,w/m^2

Boundary Surface	Heat Flux
Reactor vessel – lower vertical wall	1418.70
Reactor vessel – upper vertical wall	1937.90
Reactor vessel top	2232.20
Inner surface of containment top – inner cavity	-22.19
Inner cavity floor	-674.49
Inner cavity vertical outer boundary	-898.39
Inner vertical surface of outer containment wall	-7.50
Inner surface of containment top – outer cavity	24.28
Containment floor – outer cavity	-1.11
Inner boundary of outer cavity	-25.53
Vertical surface of SCS	-40.22
Top of SCS	-60.44
Bottom SCS	-37.10
Window	10.32
PCU top	12.57
PCU side	20.46

6.0 Transient Analysis

The objective of this analysis is to simulate a reactor vessel depressurization transient driven by a small break in the reactor vessel.

For an isentropic flow,

$$h_v = h + \frac{1}{2}u^2 \tag{1}$$

where

h_v = enthalpy of the gas in the reactor vessel (the subscript v denotes properties of the gas in the reactor vessel)
h = enthalpy of the gas at the break location
u = gas velocity at the break location

from

$$h = c_p T$$

where c_p is the specific heat under constant pressure, and T is the gas temperature, Eq. (1) gives

$$h_v - h = c_p(T_v - T)$$

and

$$u = \sqrt{2c_p\left(T_v - T\right)} \tag{2}$$

For an ideal gas,

$$T = \frac{p}{R\rho}$$

$$c_p = \frac{\gamma R}{\gamma - 1}$$

$$\gamma = \frac{c_p}{c_v}$$

where c_v is the specific heat under constant volume, and Eq. (2) gives

$$u = \sqrt{\frac{2\gamma}{\gamma - 1}\left(\frac{p_v}{\rho_v} - \frac{p}{\rho}\right)} \tag{3}$$

where

p = pressure at the break location
ρ = density at the break location
R = the ideal gas constant

For isentropic flow, the density ρ at the break is given by

$$\rho = \rho_v \left(\frac{p}{p_v} \right)^{\frac{1}{\gamma}} \tag{4}$$

If the pressure in the containment is lower than the critical pressure p_c, where

$$p_c = p_v \left(\frac{\gamma + 1}{2} \right)^{\frac{\gamma}{1-\gamma}} \tag{5}$$

then the flow is sonic and the pressure p used in Eqs. (3) and (4) is set equal to p_c, otherwise p is the pressure of the containment in the neighborhood of the break. The flow rate, w, at the break
is

$$w = A\rho u \tag{6}$$

where A is the area of the break.

Because of the depressurization, the pressure in the reactor vessel changes with time. Conservation of energy in the reactor vessel gives:

$$dE/dt = \text{enthalpy out} + \text{kinetic energy out} \tag{7}$$

where E is the internal energy of the gas in the reactor vessel. The internal energy E is

$$E = e\rho V = c_v T \rho V$$

where e is the specific internal energy and V is the reactor vessel volume. For an ideal gas

$$\rho = p/RT$$

and

$$E = c_v pV/R = \frac{pV}{\gamma - 1}$$

The reactor vessel volume is constant and

$$\frac{dE}{dt} = \frac{V}{\gamma - 1}\frac{dp_v}{dt} \tag{8}$$

The enthalpy out is

$$H_{out} = - A\rho u(e+p/\rho) = -Au(\rho e + p) \tag{9}$$

and for

$$e = c_v T, \quad \rho = p/RT, \quad c_p - c_v = R, \quad \gamma = c_p/c_v$$

Eq. 9 gives

$$H_{out} = -Aup\frac{\gamma}{\gamma - 1} \tag{10}$$

Equations 8, 9, and 10 give

$$\frac{V}{\gamma - 1}\frac{dp_v}{dt} = -Au\left(\frac{\gamma}{\gamma - 1}p + \frac{1}{2}\rho u^2\right) \tag{11}$$

Conservation of mass in the reactor vessel gives

$$V\frac{d\rho_v}{dt} = -Au\rho \tag{12}$$

Equations (3), (4), (5), (11), and (12) provide the boundary conditions for the pressurization transient of the containment that is driven by the depressurization of the reactor vessel.

Because coupling of the above equations with STAR-CD requires quite some effort, it was decided to use instead information generated by a RELAP analysis of the same transient. This information includes helium mass flow rate, temperature, pressure and internal energy at the break location. Because in this analysis a detailed simulation of the conditions in the neighborhood of the break is not of interest, and because a combination of such an analysis with the analysis in the very large containment space is computationally very demanding, the helium flow into the containment is simulated as an injection of helium in the bottom layer of computational cells adjacent to the reactor vessel. Because the cross-sectional area of these cells is much larger than the area of the break (one square inch), to simplify the analysis, the temperature and pressure of the injected gas are set equal to their stagnation values, T_{in} and p_{in}, respectively, that is:

$$T_{in} = T + \frac{u^2}{2c_p} \tag{13}$$

$$p_{in} = p\left(\frac{T_{in}}{T}\right)^{\gamma/(\gamma-1)} \tag{14}$$

where T, p, u and cp are the temperature, pressure, velocity and specific heat at the break, and

$$\gamma = c_p/c_v$$

The velocity u is computed from the mass flow rate and the pressure and temperature at the break provided by the RELAP output.

A user subroutine was written that converts the RELAP output into STAR-CD input, and a STAR transient model was developed.

To start the transient analysis, a steady state analysis was performed with reactor vessel and shutdown cooler temperatures as predicted by RELAP at normal reactor operating conditions, and a guard containment filled with nitrogen at a pressure of one atmosphere. The depressurization accident starts at the normal operating condition of the reactor plant at 100% power. This 100% steady state is therefore at the beginning of the transient whereas the long-term steady state of section 5 is at the end of the transient when a long term quasi equilibrium has been reached. These temperatures are 744 °K (471 °C) for the upper section of the reactor vessel, 752 °K (479 °C) for the lower section of the reactor vessel and 753 °K (480 °C) for the shutdown cooler (SCS). It should be noted that the steady state analysis reported earlier was based on steady state temperatures of the boundary surfaces, guard containment pressure (6 bar) and a helium concentration (mol fraction of 25 %) at the end of the transient.

Figure 21 shows the predicted temperature distribution for the guard containment walls. This distribution peaks to a value of 567 °K (294 °C) opposite to the shutdown cooler. This temperature is greatly above the concrete limiting temperature (below 373 °K (100 °C) and it is due to radiation from the hot outer walls of the shutdown cooler. At normal reactor operating conditions these walls have a much higher temperature than at the end of the depressurization transient. Insulation of the outer surface of the shutdown cooler would cut the heat transfer from the SCS to the guard containment.

Another steady state analysis was performed with the shutdown cooler insulated (adiabatic boundary condition). As Figure 22 shows, the temperature of the wall of the guard containment opposite to the cooler is drastically reduced to well below 100 °C (373 °K). However, the temperature of the guard containment above the reactor vessel remains at 131 °C, well above the concrete limiting temperature. Because this temperature is not greatly higher than the limiting temperature, it was decided to use this

steady state analysis as the initial state of the depressurization transient. This transient analysis is in progress.

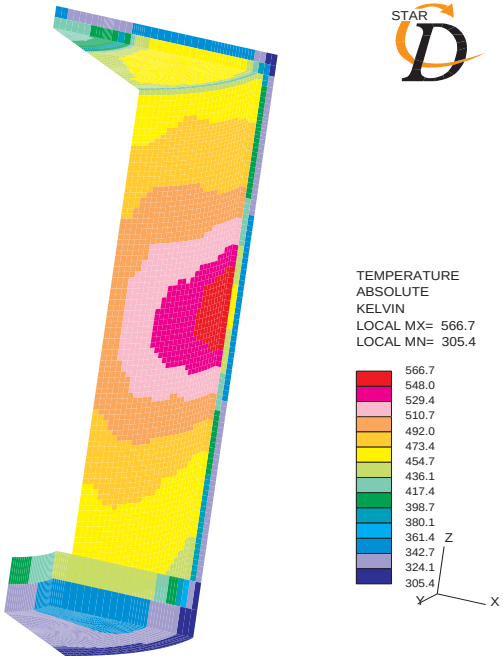

Fig. 21. Guard Containment Temperature Distribution at Initial Steady State Conditions

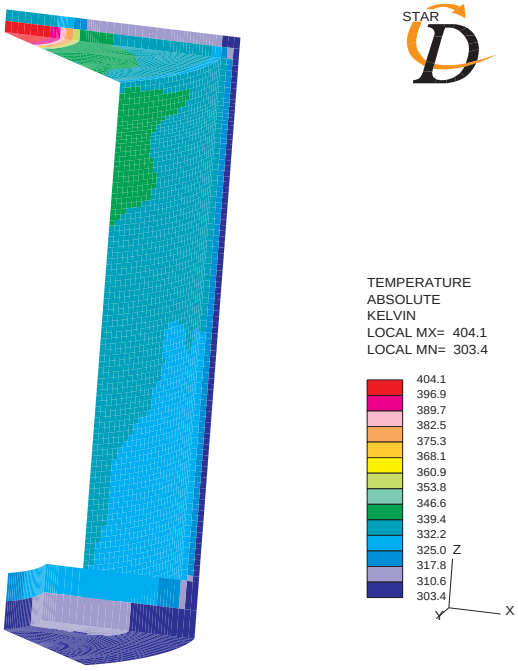

Fig. 22. Guard Containment Temperature Distribution Conditions (Insulated Shutdown Cooler.)

References

1. T. Rouault and T. Y. C. Wei, "Selection of the Concept for Point Design", I-NERI Project #2001-002-F, Report GFR 021, May 2004.
2. I-NERI Project Staff, "System Design Report", I-NERI Project #2001-002-F, Report GFR 023, February 2005.